Production of antinuclei and hypernuclei in a relativistic Hagedorn resonance gas model

Subrata Pal[1] and Walter Greiner[2]

[1]*Department of Nuclear and Atomic Physics, Tata Institute of Fundamental Research, Homi Bhabha Road, Mumbai 400005, India*

[2]*Frankfurt Institute for Advanced Studies (FIAS), J.W. Goethe-Universität, 60438 Frankfurt am Main, Germany*

(Received 7 November 2012; revised manuscript received 12 March 2013; published 15 May 2013)

We study the production of light nuclei, hypernuclei, and their antiparticles in relativistic energy heavy ion collisions from sequential decay of massive resonance states within a Hagedorn resonance gas model. The production yield of these clusters and of the multistrange hypernuclear objects are presented over a wide range of collision energies.

DOI: 10.1103/PhysRevC.87.054905 PACS number(s): 12.38.Mh, 24.85.+p, 25.75.−q

I. INTRODUCTION

The recent observation of antihelium-4 nucleus and the lightest (anti)hypernucleus and (anti)hypertitron [1,2] at the Relativistic Heavy Ion Collider (RHIC) has provided the exciting possibility of creating and studying the properties of massive antimatter nuclei and the exotic multistrange hypernuclei [3]. While the antimatter nuclei allow one to explore the negative sector of the conventional periodic table in the (N, Z) plane, the hypernuclei that consist of at least one hyperon along with the nucleons could provide additional information into the strangeness sector of the (N, Z, S) chart [4].

Studies of the production mechanism of antinuclei and hypernuclei have been mostly confined to the coalescence [5–8] and thermodynamical [9,10] models. In the microscopic coalescence calculations, (anti)nuclei are created by the overlap of the phase-space densities ρ_i of the constituent B (anti)baryons at the final stages of the dynamical evolution where the yield, $n \sim (\rho_i)^{|B|} \sim \exp(-|B|)$, is exponentially suppressed [11]. Whereas, in thermal models, the yield of nuclei with energy $E = \sum_{i=1,B} m_i$ is reduced by the Boltzmann factor $\exp(-E/T)$ with addition of each baryon [9]. The more massive and less abundant strange hyperons invoke an additional suppression factor as compared to the nucleons.

Although a large fraction of the hadrons is generated from the decay of heavy resonances, limited knowledge of the features of heavier resonances has forced one, in the thermal and transport models [8,10–12], to restrict the maximum mass of hadrons only up to the measured value of $m < 2$ GeV. Thus the growing contribution of the massive resonances to the cluster formation from direct decay or via phase-space coalescence of light hadrons has been entirely neglected.

On the other hand, Hagedorn [13] proposed that the density of hadronic states grows exponentially with resonance mass m, $\rho_{\rm HS}(m) \sim m^{-\alpha} \exp(m/T_H)$, where the Hagedorn temperature $T_H \sim 150$–200 MeV. In fact, the Hagedorn states (HS: $m \gtrsim 2$ GeV) were demonstrated to be abundantly produced in relativistic heavy ion collisions [14,15] that may lead to copious production of heavy antimatter nuclei and (multi)hypernuclei.

The massive Hagedorn states have extremely short lifetimes and these could decay rapidly into hypernuclei and antinuclei during dynamical evolution. This production mechanism is distinct to the formation at the chemical freeze-out stage in the statistical model and the kinetic freeze-out in the coalescence prescription. The produced clusters in the hot and dense medium may either decay into (anti)nuclei and hyperons with a typical lifetime of ∼10–300 ps [1] or may recombine with another particle to produce a HS which in turn can decay into (anti)clusters. Noteworthy is that the successive emission of strange hadrons in the decay chain may lead to the formation of Hagedorn states with extreme strangeness which may serve as an efficient source for the production of multistrange hypernuclear objects [3].

In this paper, we study the production of light nuclei, hypernuclei, multistrange nuclei, and their antiparticles in central heavy ion collisions from the BNL Alternating Gradient Synchrotron (AGS) center-of-mass energy $\sqrt{s_{NN}} = 2.70$ GeV to the Large Hadron Collider (LHC) energy of $\sqrt{s_{NN}} = 2.76$ TeV in the relativistic Hagedorn resonance gas (HRG) model [14,15].

The paper is organized as follows: In Sec. II, the Hagedorn resonance gas model is outlined that has been extended to include clusters. Section III contains the results and discussions. Concluding remarks are given in Sec. IV.

II. HAGEDORN RESONANCE GAS MODEL

In the HRG cascade model, a massive resonance fireball is assumed to be formed in the geometrical overlapping zone in high energy heavy ion collisions. This Hagedorn state undergoes successive binary emission relativistically into channels composed of lighter resonances (or HS), clusters, and stable hadrons. The decay chain continues till all stable particles are formed. All the low-lying measured hadrons available in the Particle Data Book have been included. During dynamic evolution, binary collisions between the particles in the HRG may regenerate the resonance thereby maintaining detailed balance. All possible $2 \leftrightarrow 2$ elastic and inelastic collision channels involving the (non)strange hadrons have been included [15]. The HRG cascade model has been extended here to include clusters. Their properties, characterized by baryon, strangeness, spin, and isospin quantum numbers $q \equiv (B, S, J, I, I_z)$, are obtained from their quark content [8]. The total mass of a hypernucleus is taken to be the sum of the masses of the constituent hadrons.

Based on the Hagedorn hypothesis [13] the density of massive states are assumed to grow exponentially with

resonance mass as

$$\rho(m,q) = A\frac{\exp[\{m - m_g f(m-m_g)\}/T_H]}{\left[\{m - m_g f(m-m_g)\}^2 + m_r^2\right]^{\alpha}}, \quad (1)$$

in the usual notation [14,15] with $m_r = 0.5$ GeV. For a mass m characterized by its quantum number q, its ground-state mass is parametrized by $m_g(q) = a_Q(\max|3B+S|, 2I) + a_S|S|$, where the parameters $a_Q = 0.387$ GeV and $a_S = 0.459$ GeV are determined empirically from the measured smallest masses.

In absence of hadronic interaction, the asymptotic $(m/T \to \infty)$ behavior of Eq. (1) entails divergence of energy, pressure, entropy for the exponent $\alpha \leqslant 7/4$, and specific heat c_V for $\alpha \leqslant 9/4$ at $T < T_H$ [16]. All these quantities diverge at any $T > T_H$. For the present study we consider $T_H = 170$ MeV which is consistent with the critical temperature T_c in the lattice QCD prediction of a crossover transition [17]. By comparing the theoretical and experimental cumulants of the spectrum [14,18] a resulting exponent $\alpha = 2.85$ has been estimated. This value suggests that the present HRG system prevents critical behavior at $T < T_H \approx T_c$ and predicts power law divergence at $T > T_H$ similar to that observed in lattice QCD studies. As $T \to T_H$ we thus encounter a regime whereby increasing the initial energy density can result in the formation of more massive hadronic resonances. Assuming that the hadronic phase is reached at $\tau \approx 2$–4 fm/c [19], then for a typical starting mass of $m \sim 100$ GeV with radius R [see Eq. (2)] [14], the initial energy density $\epsilon = m/V \approx m/(\pi R^2 \tau) \approx 0.4$–$0.7$ GeV/fm^3 corresponds to $T < T_c$ in the lattice [17]. It may be noted that the presence of massive HSs and the near critical behavior of c_V cause the speed of sound $c_s^2 = s/c_V$ and shear viscosity to entropy density ratio η/s to decrease with increasing T and reach a minima at $T_H \approx T_c$ [20,21].

Detailed descriptions of the decay widths of HS and other resonances and their formation cross section in binary collisions during dynamical evolution of the system can be found in Refs. [14,15]. We note that in the present study, which includes the (hyper)nuclei and their antiparticles, a HS (depending on its mass) may undergo decay into one of the six possible channels: (Ia) two observed discrete hadrons (DHs) of $m < 2$ GeV, (Ib) a DH and a cluster, (Ic) two clusters, (IIa) a DH and a HS, (IIb) a cluster and a HS, and (III) two HSs. For the cases (Ia–Ic), the decay width for $q \to q_1 + q_2$ is found to be [14]

$$\Gamma^{(I)} = \mathcal{C}_I \frac{(2J_1+1)(2J_2+1)p^{\star 2}(m_1,m_2)R^2}{2\pi\rho(m,q)}, \quad (2)$$

where p^* is the c.m. momentum, and $\mathcal{C}_I = \langle I_1 I_{z_1} I_2 I_{z_2} || I I_z \rangle$ refers to the Clebsch-Gordan coefficients for the isospins. For the parent HS of mass m, its characteristic radius is taken as $R \approx r_0(m/m_d)^{1/3}$ with $r_0 = 1$ fm for a $m_d = 1$ GeV hadron [14]. For the decay channel (IIa–IIb), assuming q_1 to be the discrete particle or cluster, the decay width is [14]

$$\Gamma^{(II)} = \mathcal{C}_I \frac{(2J_1+1)\, m R^2\, T_2^2\, (T_2 + m_1)}{\pi\, m_2} \frac{\rho(m_2,q_2)}{\rho(m,q)}. \quad (3)$$

Here the mass of the daughter HS is $m_2 = m - m_1$ and the effective emission temperature is $T_2 \approx T_H m_2/m$. It may be noted that this relativistic model conserves explicitly the energy momentum and quantum numbers $q \equiv (B, S, J, I, I_z)$ in each of the successive decay. Moreover, a resonance can travel relativistically with an average lifetime of $\langle\tau\rangle = \gamma/\Gamma$, where γ and Γ are, respectively, the Lorentz factor and total decay width of the resonance [14].

We have found [14] that the binary decay is dominated by the emission of a HS along with a light particle (or a cluster) via channel (3). The binary cascade model reproduces the measured hadron yield ratios at various energies from AGS to CERN Super Proton Synchrotron (SPS) energies [14,15] and also at RHIC and LHC energies (shown below). The fact that the yield ratios are also consistent with the thermal model [10,12] suggests that the hadrons in HRG may have reached chemical equilibrium. Albeit, within a rate equation approach, multimesonic collisions, $n\pi \leftrightarrow \text{HS} \leftrightarrow n'\pi + (p\bar{p}, K\bar{K}, \Lambda\bar{\Lambda}, \Omega\bar{\Omega})$ were shown to drive the strange (anti)baryons into chemical equilibrium more rapidly; the massive HS opens up the phase space for these decays [19]. The final hadron yield ratios in this model matches those in the sequential binary emission prediction. The multihadronic channels could thus influence the chemical equilibrium times and values, especially of the (multi)strange clusters. A consistent calculation of the decay widths and formation cross sections for these multimesonic reactions and their inclusion in the HRG model simulation are potentially involved and are postponed to future studies.

It is clear from Eqs. (1) and (3), that emission of a heavier mass m_1 causes an explicit Boltzmann-like suppression of $\rho(m_2,q_2)/\rho(m,q) \sim \exp\{-[m_1 + m_g(q_2)]/T_H\}$. Thus addition of each nucleon to a nucleus invokes a penalty factor due to reduction of the available density of states $\rho(m_2,q_2)$ of the daughter HS on account of its enhanced ground state mass m_g. The strange baryons in hypernuclei may entail an additional suppression from the increased m_g.

Because the yield of multistrange hypernuclei is very small, we treat them perturbatively [22–24] by neglecting the effects of their production and annihilation on the underlying collision dynamics which is dominated by the hadrons. In this approach, the multistrange hypernuclei are produced from the decay of massive HSs whenever it is energetically allowed. They are given a probability determined by the ratio of their respective partial decay widths Γ to the total decay widths of the HS. The annihilation of these nuclei by binary collisions are treated in a similar fashion by reducing their probabilities.

III. RESULTS AND DISCUSSIONS

For the Monte Carlo sequential emission of hadrons, we consider one fixed starting Hagedorn state (m_0, B_0) with strangeness S_0=0. Though the HRG model is well suited for hadron yield ratio studies, it predicts a rather narrow rapidity distribution and soft spectra for particles. Collective transverse flow effects are incorporated by considering a uniform transverse velocity distribution $d^2N/d\beta_T^2 = \Theta(\beta_T - \beta_{\max})$. In fact, the transverse mass spectra of stable (non)strange particles and antiparticles can be well reproduced for central Pb + Pb/Au and Au + Au collisions at $\sqrt{s_{NN}} = 17.2$ and 200 GeV with an average transverse velocity of $\langle\beta_T\rangle \sim 0.14c$ and $0.28c$, respectively [14]. A broad rapidity distribution for particles consistent with data can be obtained [25,26] by assuming a

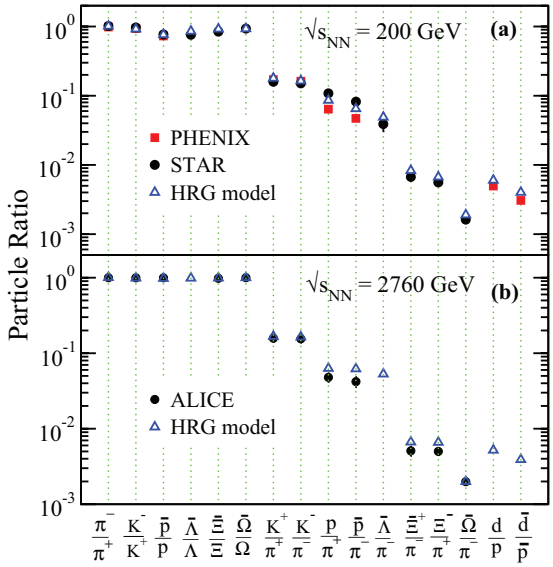

FIG. 1. (Color online) Hadron yield ratios from the HRG calculations at $T_H = 170$ MeV in central heavy ion collisions at $\sqrt{s_{NN}} = 200$ GeV and $\sqrt{s_{NN}} = 2.76$ TeV compared to the data at RHIC [29–33] and LHC [34,35].

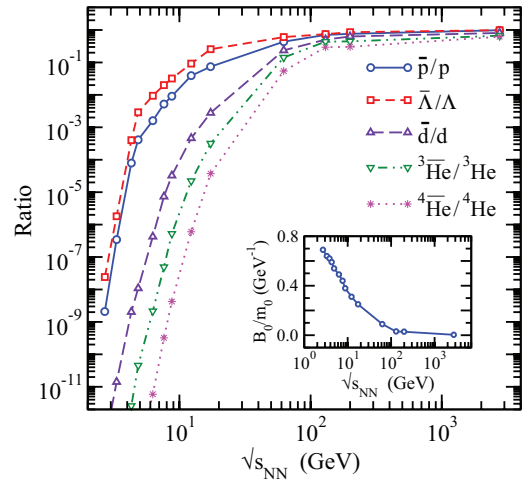

FIG. 2. (Color online) Energy dependence of the antibaryon to baryon yield ratios and B_0/m_0 ratio of the initial Hagedorn state (inset) in the HRG model at $T_H = 170$ MeV.

superposition of multiple boosted individual sources within a rapidity interval $[-y_{\min}, y_{\max}]$ so that $dN/dy = \int_{-y_{\min}}^{y_{\max}} dy'\, dN_{\rm HRG}(y - y')/dy$. Averaging over $|y'|$ corresponds to a mean longitudinal flow velocity of $\langle \beta_L \rangle = \tanh(y_{\max}/2)$. It may be mentioned that the HRG results for various hadron yield ratios is not very sensitive to the choice of $T_H = 165$–175 MeV and/or m_0 once the ratio B_0/m_0 of the initial HS is adjusted to reproduce the measured final p/π^+ or $\bar{p}/p$ ratios [14]. Further, the particle yield ratios have been shown to be insensitive to the collective motion (flow) [27] that could be generated if one considers multiple starting massive fireballs [28].

In Fig. 1, the measured particle yield ratios for central collisions in Au + Au at $\sqrt{s_{NN}} = 200$ GeV and in Pb + Pb at $\sqrt{s_{NN}} = 2.76$ TeV are compared with HRG calculations for $B_0/m_0 = 0.028$ and 0.005 GeV^{-1}, respectively. It is seen that the model calculations reproduce quite well the particle ratios involving (non)strange hadrons at the RHIC and LHC energies. As the fireball tends to be net-baryon free at the higher LHC energy, the $\bar{B}/B$ yields approach unity. The remarkable agreement for the ratios involving the lightest cluster deuteron, d/p and $\bar{d}/\bar{p}$, at the top RHIC energy suggests that this production mechanism may be extended over a wide collision energy range and for heavy clusters as well.

The inset of Fig. 2 shows the B_0/m_0 ratio of the initial fireball as estimated from the fits to p/π^+ or $\bar{p}/p$ data for central heavy ion collisions at AGS to LHC energies [14]. As expected, decrease of collision energy causes the net baryon content of the system (thus B_0/m_0) to increase appreciably. With only one such adjusted parameter B_0/m_0 and $T_H = 170$ MeV, good overall agreement with the available data for various hadron yield ratios can be obtained over this wide energy range.

Figure 2 shows the antiparticle to particle ratios over this energy range. At larger energies, near net-baryon free system induces the formation rate of antiparticles to approach that for particles. The suppression of strange particle production, especially at the lower energies, stems from phase-space reduction due to energy-momentum and event-by-event strangeness conservations invoked in the HRG model. This is in contrast to the grand canonical model where strangeness is conserved on the average [12]. It is important to note that the measured $\bar{d}/d$ ratio of ≈ 0.46 at the top RHIC energy [33] and $\sim 6.2 \times 10^{-8}$ at the AGS energy of $\sqrt{s_{NN}} = 4.85$ GeV [36] can be reproduced in the HRG, which suggests that the model may well be extended to explore large size cluster production.

The HRG results for the energy dependence of the ratios $^3\overline{\rm He}/^3{\rm He}$ and $^4\overline{\rm He}/^4{\rm He}$ are shown in Fig. 2. As seen from Table I, the calculated $^3\overline{\rm He}/^3{\rm He}$ is in excellent agreement with the STAR data at $\sqrt{s_{NN}} = 200$ GeV. Compared to the $\bar{d}/d$ abundance, an additional (anti)nucleon reduces $^3\overline{\rm He}/^3{\rm He}$ by a factor of about 1.2 at RHIC energy and the suppression could be as large as 250 times at $\sqrt{s_{NN}} = 4.85$ GeV. Addition of each (anti)nucleon to (anti)nucleus reduces the density of available states resulting in calculated yield ratios for $^4{\rm He}/^3{\rm He}$ and $^4\overline{\rm He}/^3\overline{\rm He}$ that are consistent with the RHIC data (see Table I). At the AGS energy, the large baryon content of the system gives lower (higher) penalty factor for nuclei (antinuclei) resulting in $^4{\rm He}/^3{\rm He} \approx 5.0 \times 10^{-2}$ and $^4\overline{\rm He}/^3\overline{\rm He} \approx 2.5 \times 10^{-5}$. The

TABLE I. Comparison of the particle ratios in the HRG model at $T_H = 170$ MeV with the STAR data [1,2] for central Au + Au collisions at $\sqrt{s_{NN}} = 200$ GeV.

Ratio	Data	Model
$^3\overline{\rm He}/^3{\rm He}$	$0.45 \pm 0.02 \pm 0.04$	0.44 ± 0.01
$^4{\rm He}/^3{\rm He}$	$(3.0 \pm 1.3^{+0.5}_{-0.3}) \times 10^{-3}$	2.9×10^{-3}
$^4\overline{\rm He}/^3\overline{\rm He}$	$(3.2 \pm 2.3^{+0.7}_{-0.2}) \times 10^{-3}$	2.7×10^{-3}
$^3_{\bar{\Lambda}}\overline{\rm H}/^3_{\Lambda}{\rm H}$	$0.49 \pm 0.18 \pm 0.07$	0.45 ± 0.01
$^3_{\Lambda}{\rm H}/^3{\rm He}$	$0.82 \pm 0.16 \pm 0.12$	0.43 ± 0.002
$^3_{\bar{\Lambda}}\overline{\rm H}/^3\overline{\rm He}$	$0.89 \pm 0.28 \pm 0.13$	0.48 ± 0.002

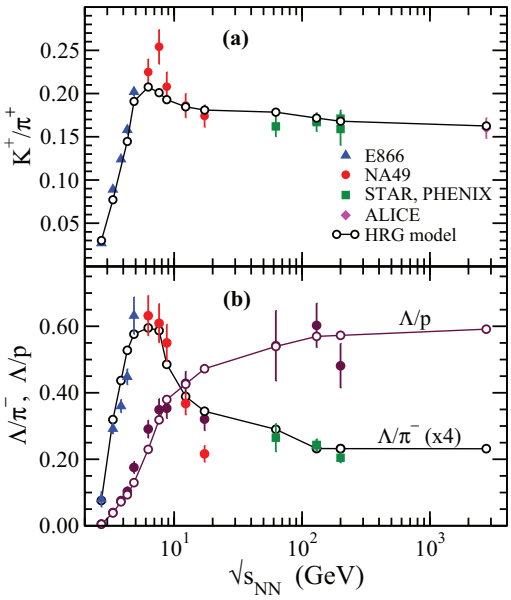

FIG. 3. (Color online) Energy dependence of the ratios K^+/π^+, Λ/π^+, and Λ/p in the HRG model at midrapidity as compared to experimental data at AGS [37], SPS [38], RHIC [29,31], and LHC [34,35].

monotonous increase of antinuclei abundance with $\sqrt{s_{NN}}$ clearly suggests that at RHIC and LHC energies reconstruction of more massive antinuclei may become feasible.

Before we present HRG estimates of the hypernuclei yield ratios, we first compare with data the model prediction for the K^+/π^+ ratio in Fig. 3(a). A maximum is seen at $\sqrt{s_{NN}} \simeq 7$ GeV, which can be understood as follows. While at the lower energies the sharp rise in B_0/m_0 (see the inset of Fig. 2) and strangeness conservation enforces strangeness suppression, at $\sqrt{s_{NN}} \simeq 10$–200 GeV the dominant emission of π (over K and K^*) from the Hagedorn states lowers the K^+/π^+ ratio. However, a careful examination reveals that HRG somewhat underpredicts the measured K^+/π^+ peak value. In fact, absence of sharp peaks in the thermal models without the HS [12,28,38,39] has led to the prediction of "the horn" as an experimental evidence for the onset of the deconfinement quark-gluon plasma transition [38,40].

As seen in Fig. 3(b), the pronounced peak in the Λ/π^- ratio and gradual increase in the Λ/p ratio are consequences of decreasing baryon density with energy and the assumption of strangeness neutrality imposed for each event in the model. The reasonable reproduction of the strange hadron yield data over a wide energy range indicates that the HRG model can be also employed to study strange cluster production.

In Fig. 4 we show the energy dependence of various cluster yield ratios in the HRG model. The lightest cluster d/p ratio is found to be in remarkable agreement with the data [33,36,41]; its steep decrease with energy reflects enhanced nucleon produced from the decay of abundant light baryon resonances. At the RHIC energy, though the HRG prediction for ${}^3_\Lambda\overline{\mathrm{H}}/{}^3_\Lambda\mathrm{H}$ ratio is consistent with the STAR data [2] (see Table I), the ${}^3_\Lambda\mathrm{H}/{}^3\mathrm{He}$ and ${}^3_\Lambda\overline{\mathrm{H}}/{}^3\overline{\mathrm{He}}$ are, however, underpredicted by about a factor of 2. In contrast, at the AGS energy, the HRG

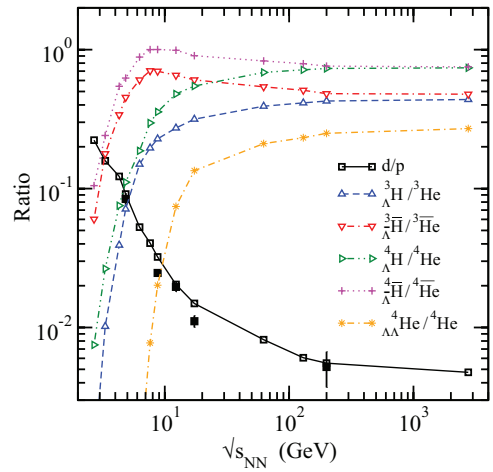

FIG. 4. (Color online) Energy dependence of hypernuclei yield ratios at midrapidity in the HRG model. Also shown is the d/p ratio in the model as compared with the data (solid squares).

predictions are seen (in Fig. 4) to be essentially similar to the measured values of ${}^3_\Lambda\mathrm{H}/{}^3\mathrm{He} \approx 0.05$ and ${}^4_\Lambda\mathrm{H}/{}^4\mathrm{He} < 0.13$ [42]. The discrepancy for these ratios at RHIC energy, also observed in the thermal model [10], may suggest a different production mechanism beyond the hadron resonance degrees of freedom. Measurements at SPS and LHC energies is thus required to pin down the possible production scenario. At $\sqrt{s_{NN}} \simeq 8$ GeV the predicted broad peaks in ${}^3_\Lambda\overline{\mathrm{H}}/{}^3\overline{\mathrm{He}}$ and ${}^4_\Lambda\overline{\mathrm{H}}/{}^4\overline{\mathrm{He}}$ are due to enhanced baryon content and strangeness neutrality that led to peaks in K^+/π^+ and Λ/π^-. The yield of baryon rich cluster ratios, such as ${}^4_\Lambda\mathrm{H}/{}^4\mathrm{He}$, are found to be systematically larger than ${}^3_\Lambda\mathrm{H}/{}^3\mathrm{He}$. This can be explained by considering Eq. (1): the penalty [via enhanced $m_g(q_2)$] for replacing a nucleon with a hyperon decreases with increasing baryon number of the hypernuclei.

Finally, in Fig. 5 we show the HRG predictions for the energy dependence of the yield of (multi)strange hypernuclei with respect to the Λ hyperon. The multistrange cluster yield is reduced both at the lower AGS energies due to strangeness

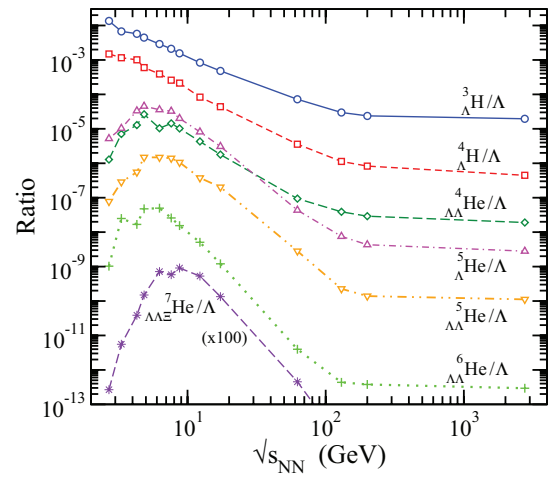

FIG. 5. (Color online) Energy dependence of the yield of hypernuclei relative to Λ at midrapidity in the HRG model.

conservation as well as at the high RHIC and LHC energies due to the small net baryon number of the fireball in spite of considerable Λ production there. At the GSI Facility for Antiproton and Ion Research (FAIR) energies, $\sqrt{s_{NN}} \approx 8A$–$20A$ GeV, most of the (multi)strange hypernuclei yield exhibits a pronounced maximum. Thus the FAIR energy seems to be the ideal regime where the search for multistrange hypernuclear objects can be focused. It may, however, be noted that due to relatively small hyperon production at this energy, the yield of doubly strange ${}^{4}_{\Lambda\Lambda}\mathrm{He}/\Lambda$ is comparable even to the baryon richer but singly strange ${}^{5}_{\Lambda}\mathrm{He}/\Lambda$. Therefore, detection of exotic multistrange hypernuclei will become increasingly difficult with larger strangeness content of the particles.

IV. CONCLUSION

We have presented the production yield of antinuclei and hypernuclei in relativistic heavy ion collisions over a wide range of beam energies within a Hagedorn resonance gas model. With a Hagedorn temperature $T_H \approx T_c = 170$ MeV, the predicted hadron yield ratios from AGS to LHC energies match the data. We find abundant antinuclei production, and their reconstruction becomes feasible at the RHIC and LHC energies where the net baryon densities are relatively small. The model agrees remarkably well with the measured yield ratios for d/p from AGS to RHIC energies and ${}^{3}\overline{\mathrm{He}}/{}^{3}\mathrm{He}$ and ${}^{3}_{\overline{\Lambda}}\overline{\mathrm{H}}/{}^{3}_{\Lambda}\mathrm{H}$ at $\sqrt{s_{NN}} = 200$ GeV. We find, however, that though the measured ratios ${}^{3}_{\Lambda}\mathrm{H}/{}^{3}\mathrm{He}$ and ${}^{4}_{\Lambda}\mathrm{H}/{}^{4}\mathrm{He}$ are well described by HRG at AGS energy, the model underpredicts these ratios by about a factor of 2 at RHIC energy, which may signify a new production mechanism. We have further shown that at $\sqrt{s_{NN}} \approx 8$–20 GeV, which is covered by the beam energy scan program at RHIC and will be also available at the FAIR facility, relatively large baryon density and moderate strangeness provide the ideal energy regime for the observation of multistrange hypernuclear objects.

ACKNOWLEDGMENT

S.P. acknowledges support from the Alexander von Humboldt Foundation and hospitality at the FIAS where part of the work was completed.

[1] B. I. Abelev *et al.* (STAR Collaboration), Science **328**, 58 (2010).
[2] H. Agakishiev *et al.* (STAR Collaboration), Nature **473**, 353 (2011).
[3] J. Schaffner, C. B. Dover, A. Gal, C. Greiner, and H. Stöcker, Phys. Rev. Lett. **71**, 1328 (1993); J. Schaffner, C. Greiner, and H. Stocker, Phys. Rev. C **46**, 322 (1992).
[4] W. Greiner, Int. J. Mod. Phys. E **5**, 1 (1996).
[5] S. T. Butler and C. A. Pearson, Phys. Rev. Lett. **7**, 69 (1961).
[6] R. Scheibl and U. W. Heinz, Phys. Rev. C **59**, 1585 (1999).
[7] J. Schaffner-Bielich, R. Mattiello, and H. Sorge, Phys. Rev. Lett. **84**, 4305 (2000).
[8] J. Steinheimer, M. Mitrovski, T. Schuster, H. Petersen, M. Bleicher, and H. Stöcker, Phys. Lett. B **676**, 126 (2009).
[9] P. J. Siemens and J. I. Kapusta, Phys. Rev. Lett. **43**, 1486 (1979).
[10] A. Andronic, P. Braun-Munzinger, J. Stachel, and H. Stöcker, Phys. Lett. B **697**, 203 (2011).
[11] S. Zhang, J. H. Chen, H. Crawford, D. Keane, Y. G. Ma, and Z. B. Xu, Phys. Lett. B **684**, 224 (2010).
[12] A. Andronic, P. Braun-Munzinger, and J. Stachel, Nucl. Phys. A **772**, 167 (2006).
[13] R. Hagedorn, Nuovo Cim. Suppl. **3**, 147 (1965); R. Hagedorn and J. Rafelski, Phys. Lett. B **97**, 136 (1980).
[14] S. Pal and P. Danielewicz, Phys. Lett. B **627**, 55 (2005).
[15] S. Pal, Phys. Rev. C **78**, 011901(R) (2008).
[16] P. Castorina, J. Cleymans, D. E. Miller, and H. Satz, Eur. Phys. J. C **66**, 207 (2010).
[17] F. Karsch, E. Laermann, and A. Peikert, Nucl. Phys. B **605**, 579 (2001); A. Bazavov *et al.*, Phys. Rev. D **80**, 014504 (2009).
[18] W. Broniowski and W. Florkowski, Phys. Lett. B **490**, 223 (2000).
[19] J. Noronha-Hostler, M. Beitel, C. Greiner, and I. Shovkovy, Phys. Rev. C **81**, 054909 (2010).
[20] J. Noronha-Hostler, J. Noronha, and C. Greiner, Phys. Rev. Lett. **103**, 172302 (2009).
[21] S. Pal, Phys. Lett. B **684**, 211 (2010).
[22] J. Randrup and C. M. Ko, Nucl. Phys. A **343**, 519 (1980).
[23] S. Pal, C. M. Ko, and Z.-W. Lin, Nucl. Phys. A **730**, 143 (2004).
[24] B. Zhang, C. M. Ko, B.-A. Li, Z.-W. Lin, and S. Pal, Phys. Rev. C **65**, 054909 (2002).
[25] E. Schnedermann, J. Sollfrank, and U. Heinz, Phys. Rev. C **48**, 2462 (1993).
[26] S. Pal, Phys. Rev. C **85**, 011901(R) (2012).
[27] J. Cleymans, H. Oeschler, and K. Redlich, J. Phys. G **25**, 281 (1999).
[28] F. Becattini, J. Manninen, and M. Gazdzicki, Phys. Rev. C **73**, 044905 (2006).
[29] J. Adams *et al.* (STAR Collaboration), Nucl. Phys. A **757**, 102 (2005).
[30] J. Adams *et al.* (STAR Collaboration), Phys. Rev. Lett. **98**, 062301 (2007).
[31] B. I. Abelev *et al.* (STAR Collaboration), Phys. Rev. C **79**, 034909 (2009).
[32] K. Adcox *et al.* (PHENIX Collaboration), Nucl. Phys. A **757**, 184 (2005).
[33] S. S. Adler *et al.* (PHENIX Collaboration), Phys. Rev. Lett. **94**, 122302 (2005).
[34] L. S. Barnby (for the ALICE Collaboration), AIP Conf. Proc. **1422**, 85 (2012).
[35] R. Preghenella (for the ALICE Collaboration), Acta Phys. Polon. B **43**, 555 (2012).
[36] T. A. Armstrong *et al.* (E864 Collaboration), Phys. Rev. Lett. **83**, 5431 (1999); **85**, 2685 (2000).
[37] L. Ahle *et al.* (E866 Collaboration), Phys. Lett. B **476**, 1 (2000).
[38] C. Alt *et al.* (NA49 Collaboration), Phys. Rev. C **77**, 024903 (2008); **78**, 034918 (2008); F. Du, L. E. Finch, and J. Sandweiss, *ibid.* **78**, 044908 (2008).
[39] J. Letessier and J. Rafelski, Eur. Phys. J. A **35**, 221 (2008).
[40] M. Gaździcki and M. I. Gorenstein, Acta Phys. Polon. **B30**, 2705 (1999).
[41] T. Anticic *et al.* (NA49 Collaboration), Phys. Rev. C **69**, 024902 (2004).
[42] T. A. Armstrong *et al.* (E864 Collaboration), Phys. Rev. C **70**, 024902 (2004).